JACS
JOURNAL OF THE AMERICAN CHEMICAL SOCIETY

Subscriber access provided by ISTANBUL TEKNIK UNIV

Article

Ag, AgS, and AgSe Nanocrystals: Synthesis, Assembly, and Construction of Mesoporous Structures

Dingsheng Wang, Ting Xie, Qing Peng, and Yadong Li

J. Am. Chem. Soc., **2008**, 130 (12), 4016-4022 • DOI: 10.1021/ja710004h

Downloaded from http://pubs.acs.org on February 8, 2009

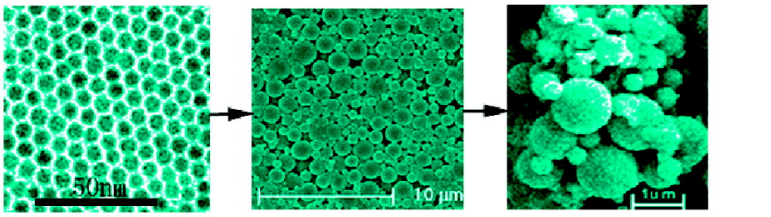

More About This Article

Additional resources and features associated with this article are available within the HTML version:

- Supporting Information
- Links to the 1 articles that cite this article, as of the time of this article download
- Access to high resolution figures
- Links to articles and content related to this article
- Copyright permission to reproduce figures and/or text from this article

View the Full Text HTML

ACS Publications
High quality. High impact.

Journal of the American Chemical Society is published by the American Chemical Society. 1155 Sixteenth Street N.W., Washington, DC 20036

J|A|C|S
ARTICLES
Published on Web 02/29/2008

Ag, Ag_2S, and Ag_2Se Nanocrystals: Synthesis, Assembly, and Construction of Mesoporous Structures

Dingsheng Wang, Ting Xie, Qing Peng, and Yadong Li*

Department of Chemistry, Tsinghua University, Beijing, 100084, P. R. China

Received November 5, 2007; E-mail: ydli@tsinghua.edu.cn

Abstract: Synthesis of mesoporous materials has become more and more important due to their wide application. Nowadays, there are two main ideas in their preparation. One is focused on the templating method. The other is based on metal−organic frameworks (MOFs) constructed from molecular building blocks. Herein, we exploit a new idea for their facile and general synthesis, namely, using "artificial atoms" (monodisperse nanoparticles) as uniform building blocks to construct ordered mesoporous materials. Mesoporous Ag, Ag_2S, and Ag_2Se have been obtained to demonstrate this concept. On the other hand, we also describe a facile method to prepare the "building blocks". Ag nanoparticles were obtained by direct thermal decomposition of $AgNO_3$ in octadecylamine, and Ag_2S/Ag_2Se nanoparticles were synthesized by reaction between sulfur or selenium powder and Ag nanoparticles formed in situ. This approach for Ag, Ag_2S, and Ag_2Se nanoparticles is efficient, economical, and easy to scale up in industrial production.

1. Introduction

Mesoporous materials have attracted considerable interest owing to their distinctive properties including high surface area, uniform pore size, and well-defined pore topology since the report of M41S by Kresge in 1992.[1] The study of their synthetic chemistry, unique structures, and novel properties has become an extremely active area in recent years which can find important applications in many fields such as catalysis, adsorption, biomolecular separation, and drug delivery.[2−4] Generally, the most popular method for mesoporous materials is focused on a template-assisted approach.[5−12] The soft templates such as triblock copolymers and surfactants or hard templates such as porous alumina and porous silica play a key role in directing the formation of porous structures. Another well-known strategy is based on metal−organic frameworks (MOFs) constructed from molecular building blocks.[13−17] The three-dimensional (3D) pore sizes and structures can be designed using various molecular struts. However, there is still a great challenge in preparing mesoporous metals and semiconductor metal chalcogenides (sulfides, selenides, and tellurides) because of the complexity in the chemical behavior of these materials, which often makes them more susceptible to hydrolysis, redox reactions, or phase transitions accompanied by thermal breakdown of the mesostructure.[18−21]

Very recently, a template-free self-assembly approach has been reported for synthesis of nanostructured Au sponges with as-synthesized Au nanoparticles as starting building blocks by Zeng's group.[22] Different from the template-assisted approach, this method avoids the hassle of template removal and promises a precise construction of 3D porous structure. Furthermore, Grzybowski and co-workers described a straightforward synthesis of macroscopic materials by a two-step method in which individual metal nanoparticles first self-assemble into deformable spherical aggregates and then "glue" together like pieces of clay into millimeter-sized structures.[23] Inspired by the work above, we developed a general strategy for the synthesis of mesoporous materials, namely, using "artificial atoms" (monodisperse nanoparticles) as uniform building blocks to construct ordered mesostructures.

(1) Kresge, C. T.; Leonowicz, M. E.; Roth, W. J.; Vartuli, J. C.; Beck, J. S. *Nature* **1992**, *359*, 710.
(2) Maschmeyer, T.; Rey, F.; Sankar, G.; Thomas, J. M. *Nature* **1995**, *378*, 159.
(3) Tanev, P. T.; Pinnavaia, T. J. *Science* **1995**, *267*, 865.
(4) Yang, P.; Deng, T.; Zhao, D.; Feng, P.; Pine, D.; Chmelka, B. F.; Whitesides, G. M.; Stucky, G. D. *Science* **1998**, *282*, 2244.
(5) Kim, T. W.; Kleitz, F.; Paul, B.; Ryoo, R. *J. Am. Chem. Soc.* **2005**, *127*, 7601.
(6) Hoffmann, F.; Cornelius, M.; Morell, J.; Fröba, M. *Angew. Chem., Int. Ed.* **2006**, *45*, 3216.
(7) Lu, Y. F.; Fan, H. Y.; Stump, A.; Ward, T. L.; Rieker, T.; Brinker, C. J. *Nature* **1999**, *398*, 223.
(8) Wan, Y.; Yang, H. F.; Zhao, D. Y. *Acc. Chem. Res.* **2006**, *39*, 423.
(9) Tian, Z. R.; Tong, W.; Wang, J. Y.; Duan, N. G.; Krishnan, V. V.; Suib, S. L. *Science* **1997**, *276*, 926.
(10) Yang, P. D.; Zhao, D. Y.; Margolese, D. I.; Chmelka, B. F.; Stucky, G. D. *Nature* **1998**, *396*, 152.
(11) Jiao, F.; Jumas, J. C.; Womes, M.; Chadwick, A. V.; Harrison, A.; Bruce, P. G. *J. Am. Chem. Soc.* **2006**, *128*, 12905.
(12) Lai, X. Y.; Li, X. T.; Geng, W. C.; Tu, J. C.; Li, J. X.; Qiu, S. L. *Angew. Chem., Int. Ed.* **2007**, *46*, 738.
(13) Russell, V. A.; Evans, C. C.; Li, W. J.; Ward, M. D. *Science* **1997**, *276*, 575.
(14) Li, H.; Eddaoudi, M.; O'Keeffe, M.; Yaghi, O. M. *Nature* **1999**, *402*, 276.
(15) Eddaoudi, M.; Moler, D. B.; Li, H. L.; Chen, B. L.; Reineke, T. M.; O'Keeffe, M.; Yaghi, O. M. *Acc. Chem. Res.* **2001**, *34*, 319.
(16) Eddaoudi, M.; Kim, J.; Rosi, N.; Vodak, D.; Wachter, J.; O'Keeffe, M.; Yaghi, O. M. *Science* **2002**, *295*, 469.
(17) El-Kaderi, H. M.; Hunt, J. R.; Mendoza-Cortes, J. L.; Cote, A. P.; Taylor, R. E.; O'Keeffe, M.; Yaghi, O. M. *Science* **2007**, *316*, 268.
(18) Braun, P. V.; Osenar, P.; Tohver, V.; Kennedy, S. B.; Stupp, S. I. *J. Am. Chem. Soc.* **1999**, *121*, 7320.
(19) Shin, H. J.; Ryoo, R.; Liu, Z.; Terasaki, O. *J. Am. Chem. Soc.* **2001**, *123*, 1246.
(20) Gao, F.; Lu, Q. Y.; Zhao, D. Y. *Adv. Mater.* **2003**, *15*, 739.
(21) Mohanan, J. L.; Arachchige, I. U.; Brock, S. L. *Science* **2005**, *307*, 397.
(22) Zhang, Y. X.; Zeng, H. C. *J. Phys. Chem. C* **2007**, *111*, 6970.
(23) Klajn, R.; Bishop, K. J. M.; Fialkowski, M.; Paszewski, M.; Campbell, C. J.; Gray, T. P.; Grzybowski, B. A. *Science* **2007**, *316*, 261.

10.1021/ja710004h CCC: $40.75 **© 2008 American Chemical Society**

Scheme 1. General Strategy for Mesoporous Materials

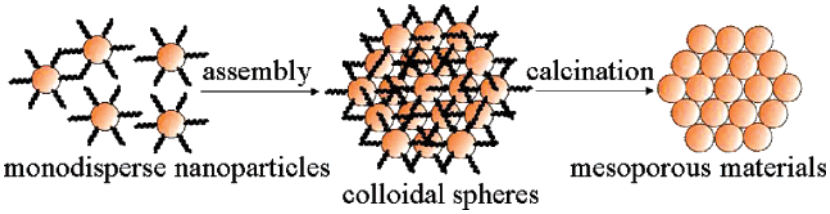

We designed the route as follows: preparation of monodisperse nanoparticles; assembly of nanoparticles with the assistance of surfactants to form 3D colloidal spheres; and calcination of these spheres to obtain mesoporous structures (Scheme 1). Actually, the method to assemble nanoparticles into desired and highly ordered architectures has been widely studied by many groups.[24−26] However, most previous methods can be applied in only one or several given products under special conditions. Comparatively, we exploited a general approach which is independent of the chemical compositions of building blocks. It allows us to obtain various kinds of mesoporous materials facilely because of the fact that the developed synthetic technology of nanometer-size crystallites makes it possible to prepare building blocks of nearly all kinds of materials.[27−37] In this paper, we take Ag, Ag_2S, and Ag_2Se as examples to demonstrate the effective process from monodisperse nanoparticles to 3D mesoporous materials.

2. Experimental Section

2.1. Synthesis of Ag, Ag_2S, and Ag_2Se Nanoparticles. All the reagents used in this work, including silver nitrate ($AgNO_3$), sulfur powder (S), selenium powder (Se), octadecylamine (ODA), ethanol, and cyclohexane, were of analytical grade from the Beijing Chemical Factory of China.

Briefly, 4.7 nm Ag particles were made by adding $AgNO_3$ (0.5 g) to solvent ODA (10 mL) at 180 °C. The mixture was magnetically stirred for 10 min in air. After reaction, particles were collected at the bottom of the beaker. For 7.3 nm Ag_2S and 8.5 nm Ag_2Se particles, we added S (0.05 g) and Se (0.12 g), respectively, into the above system after formation of Ag particles for another 10 min of magnetically stirring. All the collected products were washed several times with ethanol and then dispersed in nonpolar solvent such as cyclohexane.

2.2. Synthesis of Mesoporous Ag, Ag_2S, and Ag_2Se. A 10 mL amount of solution (the solute is Ag, Ag_2S, or Ag_2Se nanoparticles, the solvent is cyclohexane, and the concentration is about 10 mg/mL) and 0.3−0.6 g of surfactant (sodium dodecylsulfonate (SDS) or cetyltrimethylammonium bromide (CTAB)) were added to 100 mL of deionized water together. The formed system was magnetically stirred at room temperature for 1 h. After that, they were heated to 80 °C and stirred for another 1 h to evaporate the cyclohexane. The Ag, Ag_2S, or Ag_2Se colloidal spheres were obtained by centrifuging and then calcined in a furnace with a horizontal quartz tube at 300 °C for 2 h under Ar atmosphere.

2.3. Characterization of Products. Both wide- and small-angle powder X-ray diffraction (XRD) patterns were recorded with a Bruker D8-advance X-ray powder diffractometer with monochromatized Cu Kα radiation ($\lambda = 1.5406$ Å). The samples were ground and placed on a glass substrate for XRD characterization, and the 2θ range used in the measurement was from 10° to 70° for wide-angle XRD and 1.5° to 10° for small-angle XRD in steps of 0.02° with a count time of 1 s.

The size and morphology of as-synthesized samples were determined using a Hitachi model H-800 transmission electron microscope (TEM), JSM-6301F scanning electron microscope (SEM), and JEOL-2010F high-resolution transmission electron microscope (HRTEM). The specimen was prepared as follows: a small amount of product was dispersed in cyclohexane; then, one drop of the resulting suspension was transferred onto a standard holey carbon-covered copper microgrid and dried at room temperature in air.

Thermogravimetric analysis (TGA) was carried out under N_2 atmosphere at a heating rate of 10 °C/min in a temperature range from room temperature to 500 °C. N_2 adsorption/desorption isotherms were measured to determine the mesoporous structures of the samples.

3. Results and Discussion

3.1. Ag, Ag_2S, and Ag_2Se Nanoparticles. In a typical synthesis, 10 mL of ODA was added into a 50 mL beaker in air. The resulting solution was heated to 180 °C; then, 0.5 g of $AgNO_3$ was added. The color of the solution changed from colorless to light yellow and to dark brown when the mixture was magnetically stirred for 10 min, indicating formation of Ag nanoparticles. Meanwhile, we could observe that the reaction produced a mass of reddish brown gas, which might be considered as NO_2. Then, on one hand, we stopped the reaction to collect Ag product. On the other hand, we continued to add an appropriate amount of sulfur or selenium powder in the system. The color of the solution changed from brown to dark immediately, which indicated formation of the corresponding Ag_2S or Ag_2Se nanoparticles. Conversion of Ag into Ag_2S and Ag_2Se nanoparticles can be described concisely as follows

$$2\mathrm{Ag(nanoparticles)} + \mathrm{S/Se} \xrightarrow{\mathrm{ODA}} \mathrm{Ag2S/Ag2Se\ (nanoparticles)}$$

Ag particles formed in situ in this system were protected by ODA. However, when S/Se was added, the connection between Ag and N was weakened due to the much stronger interaction between Ag and S/Se. Ag_2S/Ag_2Se particles were formed and protected by ODA immediately (Scheme 2). The conversion finished so rapidly that we could not get well-defined Ag/Ag_2S or Ag/Ag_2Se core/shell particles when less than a stoichiometric amount of S/Se was used; instead, particles with a broad distribution were obtained.[38]

(24) Xu, H.; Cui, L. L.; Tong, N. H.; Gu, H. C. *J. Am. Chem. Soc.* **2006**, *128*, 15582.
(25) Sayle, D. C.; Mangili, B. C.; Klinowski, J.; Sayle, T. X. T. *J. Am. Chem. Soc.* **2006**, *128*, 15283.
(26) Zhuang, J.; Wu, H.; Yang, Y.; Cao, Y. C. *J. Am. Chem. Soc.* **2007**, *129*, 14166.
(27) Tao, A.; Sinsermsuksakul, P.; Yang, P. D. *Angew. Chem., Int. Ed.* **2006**, *45*, 4597.
(28) Tao, A.; Sinsermsuksakul, P.; Yang, P. D. *Nat. Nanotechnol.* **2007**, *2*, 435.
(29) Gao, F.; Lu, Q. Y.; Zhao, D. Y. *Nano Lett.* **2003**, *3*, 85.
(30) Murray, C. B.; Norris, D. J.; Bawendi, M. G. *J. Am. Chem. Soc.* **1993**, *115*, 8706.
(31) Peng, X. G.; Manna, L.; Yang, W. D.; Wickham, J.; Scher, E.; Kadavanich, A.; Alivisatos, A. P. *Nature* **2000**, *404*, 59.
(32) Wang, X.; Zhuang, J.; Peng, Q.; Li, Y. D. *Nature* **2005**, *437*, 121.
(33) Habas, S. E.; Lee, H.; Radmilovic, V.; Somorjal, G. A.; Yang, P. D. *Nat. Mater.* **2007**, *6*, 692.
(34) Yin, Y. D.; Li, Z. Y.; Zhong, Z. Y.; Gates, B.; Xia, Y. N.; Venkateswaran, S. *J. Mater. Chem.* **2002**, *12*, 522.
(35) Lin, X. Z.; Teng, X.; Yang, H. *Langmuir* **2003**, *19*, 10081.
(36) Hambrock, J.; Becker, R.; Birkner, A.; Weib, J.; Fischer, R. A. *Chem. Commun.* **2002**, 68.
(37) Son, S. U.; Park, I. K.; Park, J.; Hyeon, T. *Chem. Commun.* **2004**, 778.

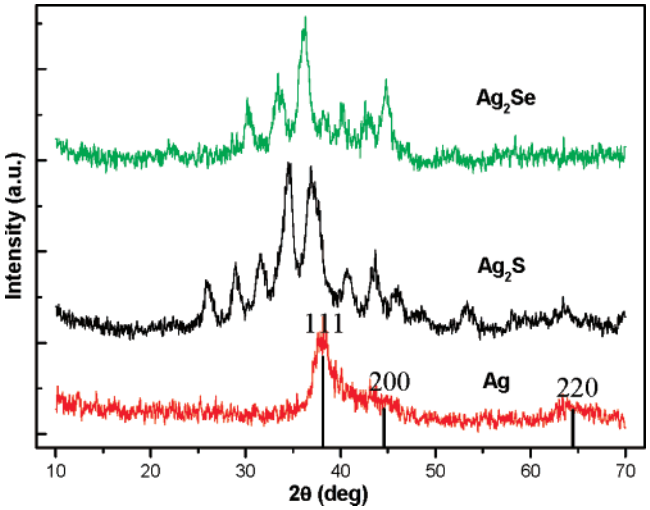

Figure 1. XRD patterns of Ag, Ag_2S, and Ag_2Se nanoparticles.

Scheme 2. Transformation of Ag into Ag_2S and Ag_2Se Nanoparticles

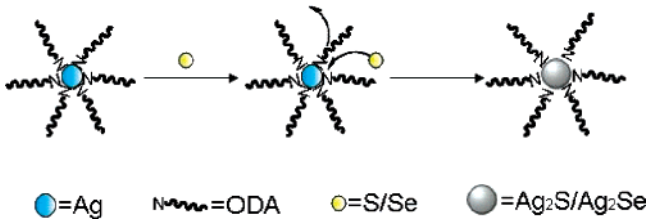

The phase identification of as-synthesized Ag, Ag_2S, and Ag_2Se nanoparticles was performed using XRD measurements (Figure 1). For Ag nanoparticles, the peaks at 38.2°, 44.5°, and 64.6° 2θ correspond to the (111), (200), and (220) reflections of face-centered cubic (fcc) structured Ag, respectively (JCPDS, 4-783).[39] For Ag_2S nanoparticles, it can be observed from the XRD pattern that monoclinic α-phase Ag_2S formed in our synthesis. All the characteristic peaks match exactly with the standard JCPDS card 14-72.[39] For Ag_2Se nanoparticles, the series of Bragg reflections in the pattern correspond to the orthorhombic Ag_2Se (JCPDS, 241041).[39] Slight peak broadening of the XRD peaks of all three kinds of nanoparticles was primarily due to the small particle size.

Their typical TEM and HRTEM images are depicted in Figure 2. The TEM images display the nearly monodisperse particle size distributions, and the HRTEM images reveal the highly crystalline nature of the nanoparticles.[40] As shown in Figure 2a, we can see that Ag nanoparticles with an average diameter of 4.7 nm could be obtained under the condition that 0.5 g of $AgNO_3$ decomposed in 10 mL of ODA at 180 °C for 10 min. These nanoparticles assembled to hexagonal packed arrays on copper TEM microgrid. Continuing to add 0.05 g of S or 0.12 g of Se into the above reaction system after formation of Ag,

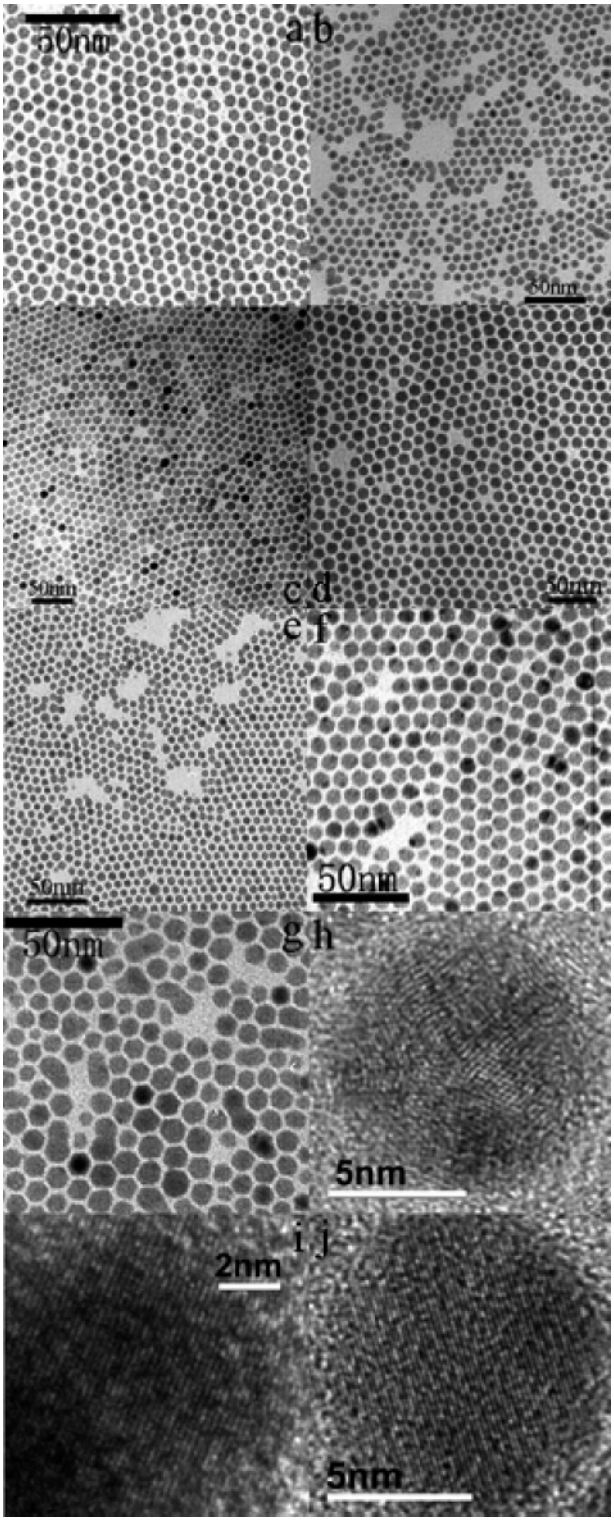

Figure 2. TEM (a−g) and HRTEM images (h−j) of as-synthesized nearly monodisperse nanoparticles: (a−e) Ag nanoparticles obtained on various conditions, (f) Ag_2S, (g) Ag_2Se, (h) Ag, (i) Ag_2S, (j) Ag_2Se.

we could get nearly monodisperse Ag_2S nanoparticles with an average diameter of 7.3 nm (Figure 2f) and Ag_2Se nanoparticles with an average diameter of 8.5 nm (Figure 2g), respectively, after another 10 min. We can also note from Figure 2f and g that the monodispersity of Ag_2Se nanoparticles is not as well as Ag_2S, which is mainly due to the much higher chemical activity of S compared to Se.

(38) See Supporting Information.
(39) Literature data on the XRD patterns for Ag: Swanson, T. Natl. Bur. Stand. (U. S.), Circ. 539, 1, 23 (1953). Ag_2S: Natl. Bur. Stand. (U.S.), Circ. 539, 10, 51 (1960). Ag_2Se: Wiegers, University Bloemsingel 10, Groningen, The Netherlands, Private Communication, 1972. The quality of the XRD pattern of Ag nanocrystals is influenced by peak broadening. However, the XRD pattern of calcined Ag spheres (see Supporting Information) can help us to further identify Ag crystal structure.
(40) Ag nanoparticles obtained in our system are five-fold multiply twinned crystals, see: Wang, Z. L. *Adv. Mater.* **1998**, *10*, 13. Wang, Z. L. *J. Phys. Chem. B* **2000**, *104*, 1153. After transformation, Ag_2S and Ag_2Se nanoparticles are monocrystals.

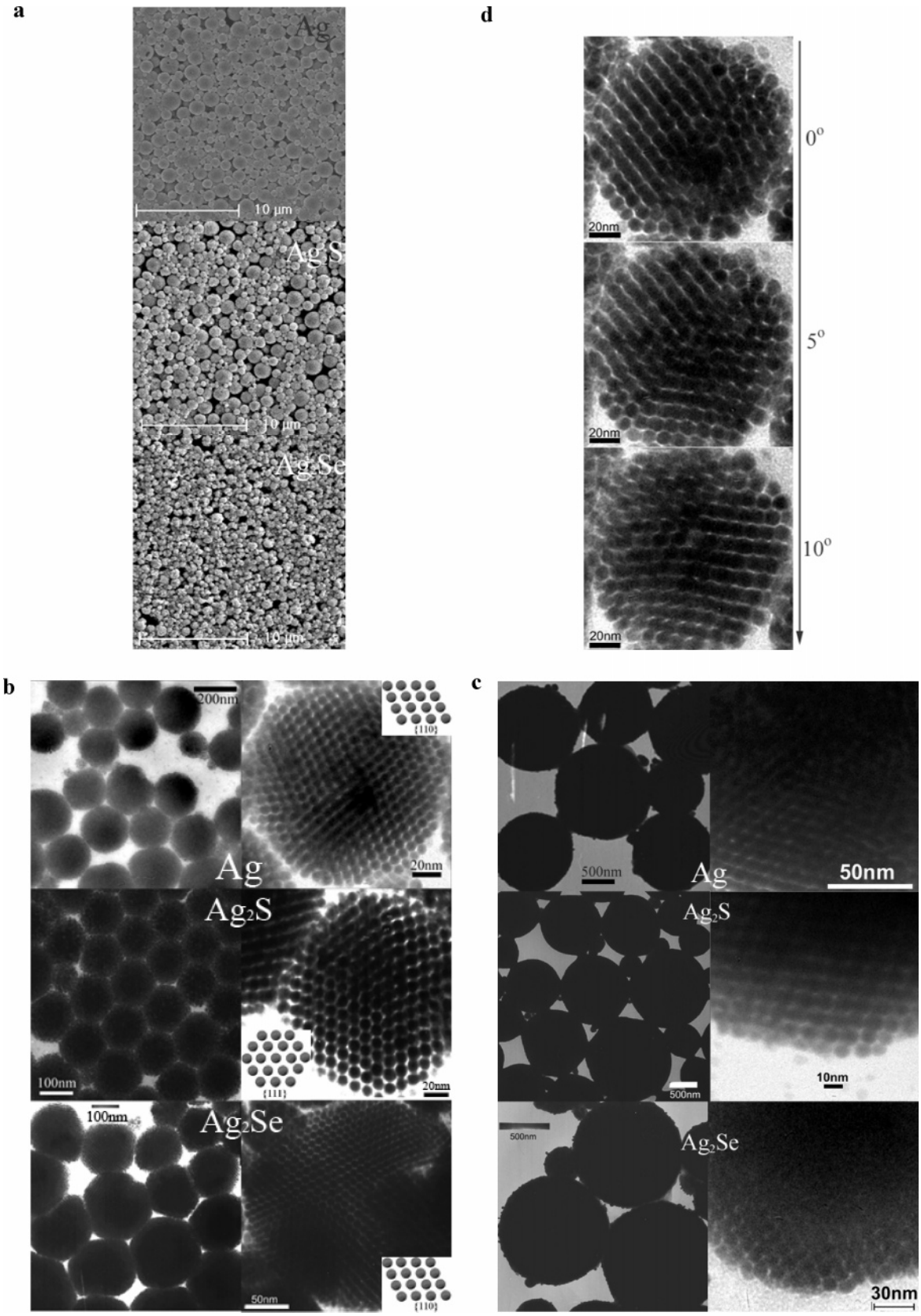

Figure 3. SEM, TEM, and HRTEM images of as-obtained colloidal spheres: (a) SEM images of Ag, Ag_2S, and Ag_2Se. (b) TEM and HRTEM images of a well-ordered superlattice with small size. (c) TEM and HRTEM images of a well-ordered superlattice with large size. (d) A series of HRTEM images of the rotation of an individual well-ordered Ag_2S spherical crystal.

The particle size can be easily controlled by tuning the reaction parameters, for example, the reaction time. Figure 2b and c shows the TEM images of Ag nanoparticles obtained on condition that 0.5 g of $AgNO_3$ decomposed in 10 mL of ODA

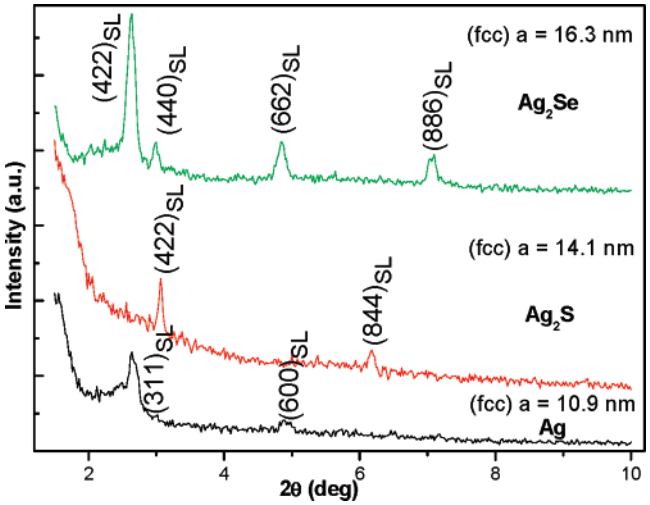

Figure 4. Small-angle X-ray diffraction patterns of Ag, Ag_2S, and Ag_2Se colloidal spheres.

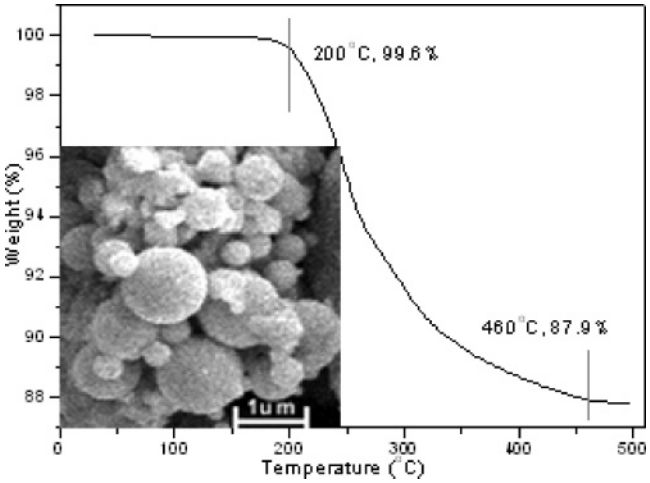

Figure 5. TGA curve of Ag colloidal spheres, and the inset shows a SEM image of calcined Ag sample (mesoporous Ag).

at 180 °C for 30 and 60 min, respectively. The average diameters of Ag nanoparticles increased from 6.6 to 8.6 nm when the reaction time was increased from 30 to 60 min. In addition, the as-described process for nanoparticles can be scaled up facilely without changes in quality of particles or reducing of product yield. For example, when 5 g of $AgNO_3$ was added into 100 mL of ODA at 180 °C, Ag nanoparticles could be also obtained after 60 min of magnetically stirring (Figure 2d). From Figure 2c and d, it can be noted that the size of Ag nanoparticles synthesized in large scale stays nearly unchanged, and the particles are also narrowly dispersed. Furthermore, the solvent ODA used in our synthesis is testified to be recycled. After the final products were collected at the bottom of the beaker, the residual ODA can be used for the next synthesis. Figure 2e shows the TEM image of Ag nanoparticles with nearly the same size and monodispersity as Figure 2a, which were synthesized with the recycled ODA. The above advantages promise its tremendous potentiality in industrial production of nearly monodisperse Ag, Ag_2S, and Ag_2Se nanoparticles.

3.2. From Monodisperse Nanoparticles to 3D Mesoporous Materials. After we obtained the nanoparticles, a surfactant-assisted self-assembly process was carried out to obtain their corresponding colloidal spheres with well-ordered 3D superlattice structures.[41] Microemulsion oil droplets were used as confined templates. The oil phase contained presynthesized well-dispersed Ag, Ag_2S, and Ag_2Se nanoparticles encapsulated in ODA and aqueous solution containing SDS or CTAB. Because the size of oil droplets formed in situ in microemulsion could not be uniform on condition of mechanical stirring, the as-obtained colloidal spheres are polydisperse whose diameters range from 100 nm to 2 μm. The SEM images (Figure 3a) give us a whole view of the morphology and size of the samples. However, we can separate them by centrifugation at different rotation speeds because there are obvious differences in the mass among various-sized spheres.

Figure 3b and c shows the TEM and HRTEM images of small and large spheres separated by centrifugation, respectively, from which we can see clearly that Ag, Ag_2S, and Ag_2Se nanoparticles have assembled to colloidal spheres effectively with the assistance of surfactants and no separate particles are found. The average size of the small spheres in Figure 3a is 200 nm for Ag, 100 nm for Ag_2S, and 200 nm for Ag_2Se.[42] Their corresponding HRTEM images exhibit well-ordered superlattice structures. To illustrate that the samples are not 2D ordered superstructures, we carried out the rotation experiment of HRTEM. Take Ag_2S as an example, Figure 3d shows the experimental results. The orientation of Ag_2S arrays changed with the increase of the angle, which confirms that the samples are true 3D spherical superlattice structures. From Figure 3c, we can see that the average size of large spheres is 1 μm for Ag, 1.2 μm for Ag_2S, and 1.1 μm for Ag_2Se. In their corresponding HRTEM images, it is noted that the bodies become gradually darker from the edge to the center, which also indicates the 3D structures of the samples. We can deduce the whole bodies present superlattice structures from the ordered arrangement of nanoparticles in the edge.

The symmetry and structure of Ag, Ag_2S, and Ag_2Se 3D superlattices were further determined by small-angle X-ray diffraction (SAXRD, Figure 4). For Ag, the two peaks correspond to d spacings of 33 and 18 Å. These peaks display d-value ratios of $\sqrt{11}:\sqrt{36}$, which can be indexed as (311) and (600) reflections, respectively, in a face-centered cubic (fcc) superlattice structure with a lattice constant of about 10.9 nm.[38] For Ag_2S, the two peaks can be indexed as (422) and (844) reflections, respectively, in a fcc structure and the lattice constant is about 14.1 nm.[38] For Ag_2Se, there are four peaks corresponding to (422), (440), (662), and (886) reflections in a fcc structure with $a = 16.3$ nm.[38] On the other hand, HRTEM (Figure 3b) clearly shows that all three kinds of particles exhibit a fcc superlattice structure. The images of Ag and Ag_2Se are viewed along the [011] zone axis, and that of Ag_2S is viewed along the [111] zone axis (Figure 3b, inset). The lattice constant measured from HRTEM is also consistent with the analytical results from SAXRD.[38]

(41) Bai, F.; Wang, D. S.; Huo, Z. Y.; Chen, W.; Liu, L. P.; Liang, X.; Chen, C.; Wang, X.; Peng, Q.; Li, Y. D. *Angew. Chem., Int. Ed.* **2007**, *46*, 6650.

(42) The as-obtained colloidal spheres are polydisperse with size from 100 nm to 2 μm. The TEM images here show only part of the spheres. Actually, Ag_2S nanoparticles can also assemble into superlattices with a diameter of 200 nm.

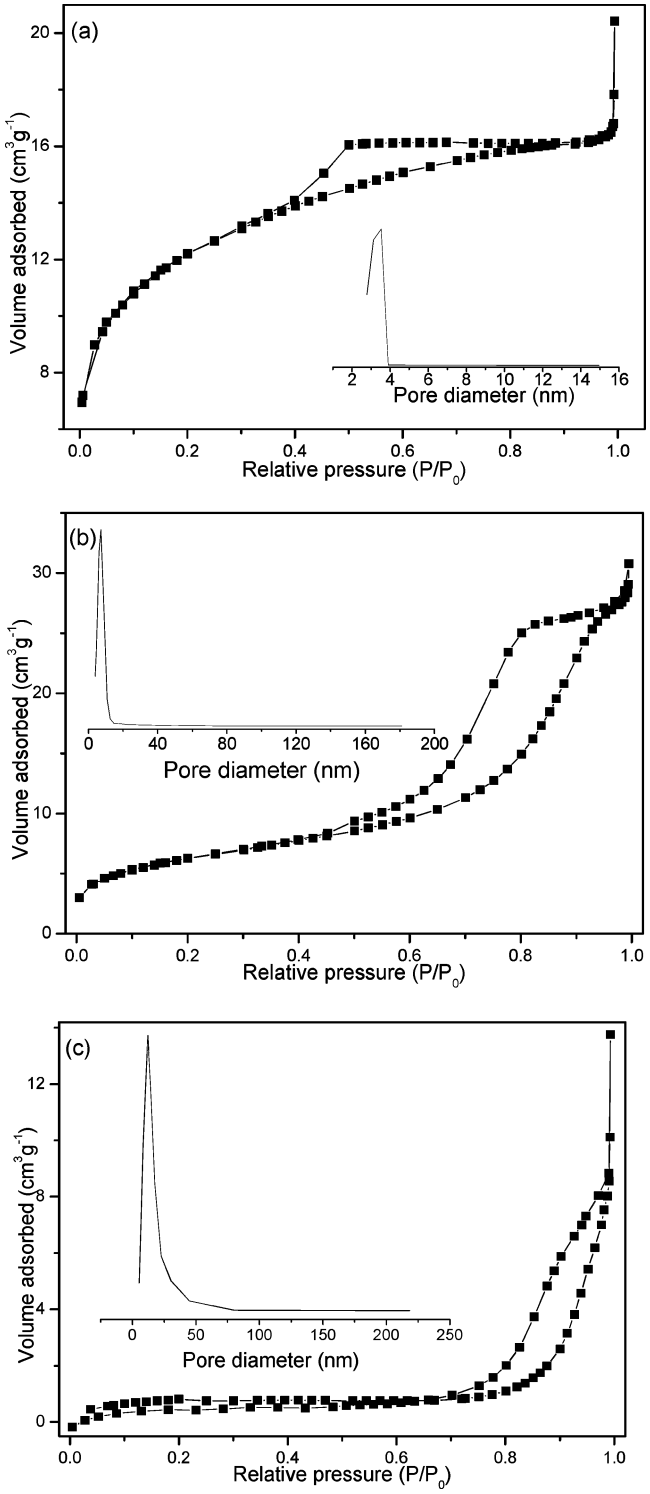

Figure 6. N_2 adsorption−desorption isotherm and corresponding pore size distribution curve (inset) for as-synthesized mesoporous materials: (a) Ag, (b) Ag_2S, (c) Ag_2Se.

In order to gain mesoporous structures finally, surfactants were removed by calcination under an argon atmosphere. XRD measurement was used to determine the composition of the calcined products. For Ag_2S and Ag_2Se, combustion leads not only to ODA removal but also to their partial decomposition into Ag and S and Se. For Ag, it can keep the composition.[38] Figure 5 shows the TGA curve of Ag colloidal spheres, from which only one weight-loss step can be observed. This step is from 200 to 460 °C, corresponding to combustion of surfactants. The sphere morphology can be well maintained during this process (Figure 5, inset), which leads to formation of mesoporous structures. N_2 adsorption/desorption analysis was used to examine these mesostructures, and the data are shown in Figure 6. The Barrett−Joyner−Halenda (BJH) pore-size distribution curves (Figure 6, insets) indicate that the as-obtained three kinds of mesoporous materials exhibit a narrow pore-size distribution, and their average pore diameters are 3.5, 7.2, and 12 nm. We can explain the difference among the pore sizes of the three kinds of mesoporous spheres through rough calculation. As discussed above, the accumulated particles show fcc structure and the lattice constant can be determined. In every unit cell, the volume occupied by solid particles is $16\pi R^3/3$ (R = radius of the particle) and the pore volume can be determined as $a^3 - 16\pi R^3/3$ (a = the lattice constant).[38] If we assume that the pore is spherical, we can calculate the pore size with eq 1 roughly[38]

$$r = \sqrt[3]{\frac{3}{16\pi}\left(a^3 - \frac{16\pi R^3}{3}\right)} \text{ (r: radius of the pore)} \quad (1)$$

When R increases, a also increases. From our experimental results, it can be seen that the ratio of a to R is nearly 4:1.[38] Then, the relationship between r and R can be described as follows

$$r \approx \sqrt[3]{\frac{3}{16\pi}\left((4R)^3 - \frac{16\pi R^3}{3}\right)} = \sqrt[3]{\frac{3}{16\pi}\left(64 - \frac{16\pi}{3}\right)} R \propto R$$

Thus, we can qualitatively consider that the pore size will increase with increasing diameter of the building blocks. At the same time, according to the literature,[23] the surface area of the porous materials will decrease when the diameter of the building blocks increases, as evidenced by our experimental results. The corresponding Brunauer−Emmett−Teller (BET) surface areas for the three kinds of mesoporous materials are 43.2, 22.9, and 3.1 $m^2\ g^{-1}$.

4. Summary

In conclusion, on one hand, nearly monodisperse Ag, Ag_2S, and Ag_2Se nanoparticles have been synthesized. Compared to some commonly used procedures, this approach shows at least three advantages. First, the process is very facile and economical. Then, this reaction can yield nanoparticles in a large amount with high productivity, and it can be scaled up easily. Furthermore, the solvent ODA is testified to be recycled. On the other hand, these as-obtained nanoscale particles have been used as uniform building blocks to successfully construct well-ordered mesoporous structures. This is a general and powerful strategy for preparation of mesoporous materials. It is foreseeable that mesoporous structures of other metals, semiconductors, fluorides, and phosphides can also be synthesized by a similar process, and we can regulate their pore sizes which depend on sizes of corresponding nanoparticles. More importantly, due to the novel structure and high porosity of the mesoporous materials, they can find significant applications in various fields such as catalysis, adsorption, separation, etc.

Acknowledgment. This work was supported by NSFC (90606006), the Foundation for the Author of National Excellent Doctoral Dissertation of China and the State Key Project of Fundamental Research for Nanoscience and Nanotechnology (2006CBON0300), the Key grant Project of the Chinese Ministry of Education (NO.306020).

Supporting Information Available: Detailed analytical data, XRD patterns, and TEM image. This material is available free of charge via the Internet at http://pubs.acs.org.

JA710004H